Mon. Not. R. Astron. Soc. **000**, 000–000 (0000) Printed 9 April 2013 (MN LATEX style file v2.2)

Multi-wavelength Observations of the Giant X-ray Flare Galaxy NGC 5905 : signatures of tidal disruption

H.Raichur[1], M.Das[2], A.Alonso Herrero[3], P.Shastri[2], N.G.Kantharia[4]

1. Raman Research Institute, Bangalore, India.
2. Indian Institute of Astrophysics, Koramangala, Bangalore 560034, India.
3. Instituto de Fisica de Cantabria, CSIC-UC, Avenida de los Castros S/N, ES 39005 Santander, Spain.
4. National Centre of Radio Astrophysics, TIFR, Pune, India.

Accepted.....; Received .....

ABSTRACT

NGC 5905 is one of the few galaxies in which an X-ray flare was discovered by the ROSAT All Sky Survey (RASS). This flare was supposed to have occurred due to tidal disruption of a star by the central black hole. In this work we present analysis of multi-wavelength follow-up observations made in X-ray, mid-infrared and radio using data obtained from the Chandra X-ray observatory, Spitzer and Giant Meter wave Radio telescope (GMRT) respectively. The archival Chandra 2007 observations show that the X-ray luminosity in the energy band of 0.5-2.0 keV has decreased by a factor of 200 since the peak of the X-ray flare observed in 1990. The X-ray image reveals no centrally bright core expected in the presence of an AGN. Diffuse X-ray emission lying close to the circum-nuclear star forming ring is observed. The radio flux density observed with the GMRT data is similar to the flux density derived using the VLA FIRST observation in 1997 which indicates that the radio emission is probably unaffected by the 1990 X-ray flare. The archival Spitzer 2006 mid-infrared spectrum shows strong evidence of nuclear star formation but does not show any clear signatures of AGN activity. Therefore, we conclude, that there is no central AGN in NGC 5905 and reaffirm that the 1990 X-ray flare observed in this galaxy was a tidal disruption event and not due to AGN variability. NGC 5905 represents one of the few direct evidences that non-accreting black holes exist and hence provides an opportunity to study the post-outburst evolution of a tidal disruption event in the nucleus of a giant low surface brightness galaxy.

Key words: Galaxies:spiral - Galaxies:individual (NGC 5905) - Galaxies:nuclei - Galaxies:X-ray - Galaxies:active - X-rays - radio continuum - infrared radiation.

1 INTRODUCTION

NGC 5905 is a barred spiral galaxy (SB(r)b type) at a distance of 47.8 Mpc (z=0.011 and H_0=73 km s^{-1} pc^{-1}). It is classified as a giant low surface brightness (GLSB) galaxy because of its low surface brightness disk (Kent 1985; Sprayberry et al. 1995). Like most GLSB galaxies, the HI disk is very extended and relatively poor in star formation (van Moorsel 1982) even though it is interacting with the nearby galaxy NGC 5908. This interaction has resulted in the formation of extended spiral arms and a bar in the galaxy center. This galaxy also has a relatively bright bulge and shows nuclear star formation. Optical observations in Hα of the nucleus of this galaxy reveal a circum-nuclear ring of star formation of $\approx$ 1 kpc in diameter (Mazzuca et al. 2008; Comeron et al. 2010).

Active Galactic Nuclear (AGN) activity in late type galaxies such as GLSB galaxies, is relatively weak in comparison to the activity observed in other early-type galaxies (Ho 2008). Recent studies of large LSB galaxies suggest that they lie below the M-σ correlation for bright galaxies (Pizzella et al. 2005). X-ray observations reveal that these galaxies do not follow the usual radio–X-ray correlation (Das et al. 2009) and indicate that probably the central black hole (BH) masses of these system are lower than the masses of their counterpart in other normal galaxies (Ramya et al. 2011; Naik et al. 2010). The lower mass of the central BH is probably due to the fact that there is not enough gas infall towards the nuclear regions of these galaxies to fuel the growth of the super massive black hole (SMBH, Norman & Silk 1983). Gas infall is triggered by disk perturbations such as bars and spiral arms but these features are difficult to form in LSB galaxies because of their massive dark matter halos (Mayer & Wadsley 2004; Kuzio de Naray et al. 2008; Walker et al. 2010).

ROSAT All-sky survey (RASS) discovered an X-ray flare in NGC 5905 in 1990. During the X-ray flare the soft X-ray luminosity reached a peak of $L_X \sim 6 \times 10^{41}$ ergs s^{-1} (assuming an absorbed powerlaw spectral model with $N_H = 1.5 \times 10^{20}$ cm^{-2}, a power law index of 4 and distance 47.8 pc) and decreased below 9×10^{40} ergs s^{-1} within 5 months of the X-ray outburst (Bade et al. 1996). Very few cases of X-ray outbursts of variability amplitude greater than 80 have been observed (Donley et al.

Table 1. Details of Observational Data

Wave-length	Instrument	Date of Observation	Exposure time
X-ray	ACIS-S	2002-10-04 00:47:57	9.980 ks
		2007-06-07 09:26:01	44.95 ks
		2007-06-09 01:50:39	26.95 ks
Radio	GMRT 1278 Hz	June 2011	2 hours
	VLA FIRST	May 1997	....
	VLA 8 GHz (archive)	November 1996	45 min
IR	Spitzer/IRS	2006-01-16 13:46:48	SH 30s × 2 cycles
			LH 60s × 2 cycles

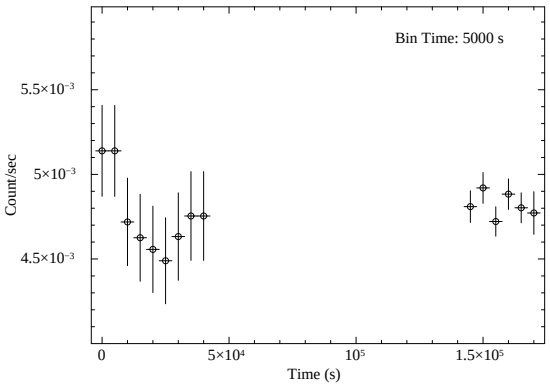

Figure 1. The first and second segment of the above light curve were extracted using data from Obs-Id 7728 and Obs-Id 8558 respectively. There is no detectable variability during these observations when the dithering effect is taken into account.

2002; Esquej et al. 2007; Saxton et al. 2012a; Maksym et al. 2010). Follow-up X-ray observations using ROSAT and Chandra show that the X-ray luminosity of the galaxy declined as $L_x \propto t^{-5/3}$, as expected in the event of tidal disruption of a star near the central BH (Rees 1988; Komossa & Bade 1999; Halpern et al. 2004). Using the stellar velocity dispersion in the bulge of NGC 5905 ($\sigma = 174.6 \pm 9.0$km/s Ho et al. 2009) and the $M_{BH} - \sigma$ calibration (Gültekin et al. 2009), the calculated mass of the nuclear BH in NGC 5905 is $M_{BH} \sim 10^7\ M_\odot$. This is consistent with the upper limit of $M_{BH} = 10^8\ M_\odot$ derived by assuming that the 1990 X-ray flare was due to tidal disruption of a star (Halpern et al. 2004). Hence the nucleus of NGC 5905 may have a SMBH of mass not greater than $10^7\ M_\odot$, which is the upper limit for black hole masses observed in LSB galaxies (S.Subramanium et al. 2013, in preparation).

Ground based optical observations of NGC 5905 classified the nucleus as an H II or starburst galaxy (Giuricin et al. 1990, Ho et al. 1995). However, post-outburst Hubble Space Telescope/Space Telescope Imaging Spectroscopy (HST/STIS) observations of this source place it in the low luminosity Seyfert 2 category (Gezari et al. 2003). However, they neither found any broad Balmer line emission nor any direct evidence for a non-stellar continuum in the observed spectrum. They also could not explain the observed emission lines as due to photoionization of clouds surrounding the central BH illuminated by the soft X-ray flare observed in 1990. This raised some doubts about the origin of the X-ray flare, whether it is due to tidal disruption of a star by the SMBH or due to variability in the low-luminosity Seyfert nucleus. Thus it is important to establish the nuclear nature of NGC 5905.

In this paper, we analyze multi-wavelength observations of NGC 5905, to understand and constrain the nuclear properties of the galaxy. Only few cases of tidal disruption events in non-active galaxies have been discovered (Bower et al. 2013; Esquej et al. 2012; Saxton et al. 2012b; Cappelluti et al. 2009; Gezari et al. 2009, 2008). Detecting stellar disruption events due to the tidal field of a quiescent black hole is one of the few methods by which we can probe non-accreting SMBHs in the nuclei of galaxies. Otherwise, AGN activity is generally used to study SMBHs in distant galaxies. In § 2 we give the details of the multi-wavelength data used in this work and its analysis. In § 3 we present the results of our analysis and their implications and finally conclude our findings in § 4.

2 OBSERVATIONS AND ANALYSIS

2.1 Chandra X-ray observations

NGC 5905 was observed using the Advanced CCD Imaging Spectrometer (ACIS) on board the Chandra X-ray telescope in 2002 (Obs-Id: 3006 used in Halpern et al. 2004) and in 2007 (Obs-Id: 7728, 8558). Table 1 gives the details of the observations. Sometimes large flares are detected in the ACIS background light curve and if such flares are detected during the observation then data recorded during the background flares should be filtered[1]. During the 2002 observation, large flares were detected in the background light curve and filtering out these events resulted in a total usable exposure time of only 3.2 ks. Furthermore NGC 5905 was not detectable in the image extracted from this filtered data. Hence we do not use Obs-Id 3006 for further analysis presented in this work. No background flares were detected in the ACIS background light curves extracted from the 2007 observations.

Chandra data was used to extract (a) the X-ray light curve of NGC 5905, (b) the image of NGC 5905 in two X-ray energy bands, (c) the X-ray spectrum of the central region and (d) the image of diffuse X-ray emission. We first examined the source light curve for X-ray flux variability using the Chandra task `glvary`. The source light curve extracted using `glvary` takes into account the variability due to dithering and optimizes the bin time for the light curve accordingly. A quick look at the light curve shown in Figure 1 shows no count rate variability. From the results of `glvary` we find that the probability that the observed signal is variable is 0.2 and the variability index is 0 implying that no variability was observed during the 2007 observations of NGC 5905.

Since the source flux did not vary during the two observations of 2007, we merged the events obtained from both the pointings and made a combined image of NGC 5905 with better statistics in two energy bands namely 0.5-2.0 keV and 2.0-7.0 keV. Before merging the events, we matched the aspect solution of Obs-Id 8558 to that of Obs-Id 7728 using an X-ray point source in the field of view located at RA:15:15:18.254 and Dec:+55:32:53.71. Since both the observations have similar pointing offsets of 0.005', the shift is very small, ΔRA $= 8.63 \times 10^{-6}$ deg and ΔDec $= -1.52 \times 10^{-5}$ deg, corresponding to a physical shift in x-direction of -0.06 pixels and in y-direction of -0.11 pixel. After reprojecting the events to a different tangent point using the matched aspect solution, combined images in the two energy bands were extracted using the task `fluximage`. Figure 2 shows the image of NGC 5905 in the two energy bands. No central peak near or at the location of the optical center is seen in either of the X-ray images and NGC 5905 is hardly discernible above the background in the (2.0-7.0) keV energy image.

[1] Chandra memo for ACIS background flares

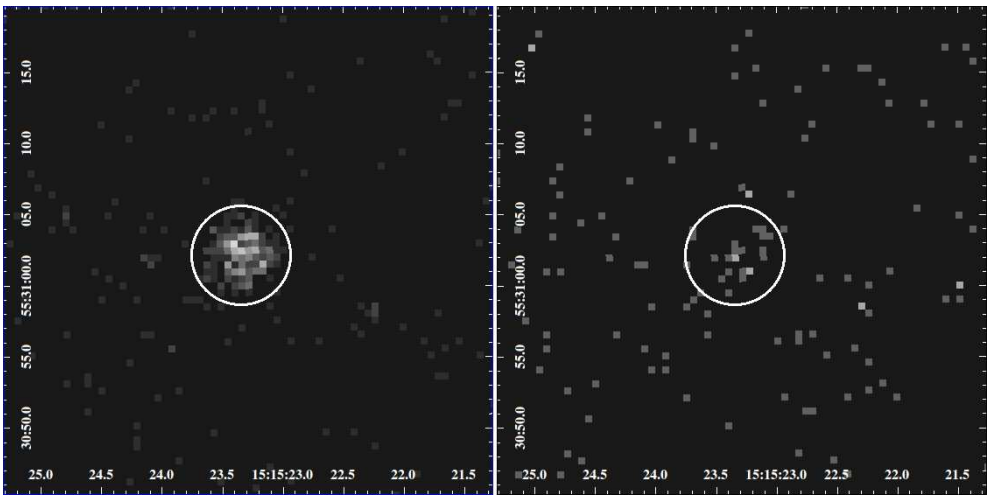

Figure 2. Image of NGC 5905 in the energy band 0.5-2.0 keV (left panel) and 2.0-7.0 keV (right panel) is shown. No centrally bright pixel is seen in either of the images. The circle marks the region from which the X-ray spectrum is extracted.

Table 2. Parameters of the X-ray spectrum model

Model			Component I		Component II					
	N_H	Γ	Norm	kT	Norm	χ^2	dof	$L_{x(0.5-2\ keV)}$	$L_{x(2-7\ keV)}$
	(10^{22}cm^{-2})		photons cm^{-2} keV^{-1}	keV				erg s^{-1}	erg s^{-1}
wabs(pwlw+bb)[a]	$0.71^{0.48}_{-0.38}$	$3.29^{2.01}_{-1.85}$	$7.34^{2.38}_{-6.19}\times10^{-6}$	$8.53^{0.04}_{-0.02}\times10^{-2}$	$2.96^{264}_{-2.82}\times10^{-5}$	12.79	11	(3.2±0.3)×10^{39}	(7.1±4.8)×10^{38}
wabs(pwlw)[a]	$0.67^{0.36}_{-0.25}$	$6.79^{2.47}_{-1.71}$	$3.87^{6.44}_{-2.05}\times10^{-5}$	–	–	25.74	13	(3.1±0.3)×10^{39}	(1.05±0.09)×10^{37}
wabs(bb)[b]	0.17	–	–	0.17	4.33×10^{-7}	31.44	13	3.11×10^{39}	2.48×10^{37}
wabs(bb)[b]	0.015 (fixed)	–	–	0.22	1.90×10^{-7}	35.41	14	3.06×10^{39}	7.81×10^{37}

[a] Fixing the N_H value to the Galactic $N_H = 1.5\times10^{20}$cm^{-2} gives a bad fit with $\chi^2_\nu > 2$
[b] Reduced χ^2 is greater than 2 and hence no uncertainties on the fitted parameters can be calculated

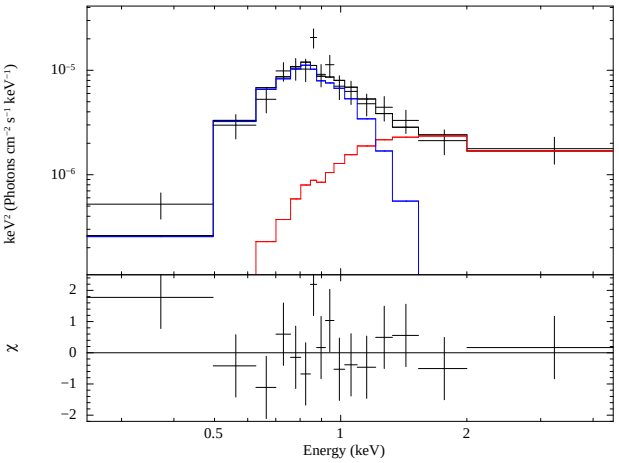

Figure 3. The X-ray spectrum of NGC 5905 extracted from the region marked in figure 2 along with the best-fit model (black curve) and the χ residuals (lower panel). The model consists of an absorbed powerlaw (red curve) and a blackbody (blue curve) component. See Table 2 for the model details.

The spectrum of NGC 5905 is extracted from a circular region of 3.5" radius, shown in Figure 2. We extracted the spectra and responses separately for the two pointings and then co-added them to get a final combined spectrum. Corresponding background spectra were extracted from a source free region on the CCDs. The spectra and corresponding responses were extracted using the task `specextract` and coadded using the task `combine_spectra`. We grouped the combined spectrum such that each energy bin has 15 counts. Figure 3 shows the spectrum of NGC 5905 with the best fit model.

To derive the diffuse emission in NGC 5905 we used the field of view of CCD-Id: 7 and included only events in the energy band of 0.5-7.0 keV. First, sources in the field of view were detected using `wavedetect` and then separate source and background region files for the detected sources were created using `roi` and `splitroi`. The source count rates were replaced by corresponding background counts for each source region and an image for each pointing was created by `dmfilth`. Images and exposure maps, thus created for each pointing, were combined using the tasks `reproject_image_grid` and `reproject_image`. The combined diffuse emission image was first exposure-corrected and then divided by the exposure map to produce the required flux image. We detected weak, diffuse emission near the nucleus of NGC 5905. The peak emission has a value approximately 14 times the background emission and this emission lies close to the circumnuclear ring of star formation, as shown in Figure 4, where the contours of the diffuse emission are overlaid on the Hα image which is obtained from the Atlas of Images of NUclear Rings (AINUR, Comeron et al. 2010).

2.2 Radio observations

NGC 5905 was observed during June 2011 in radio continuum at 1280 Hz using the Giant Metrewave Radio Telescope (GMRT)

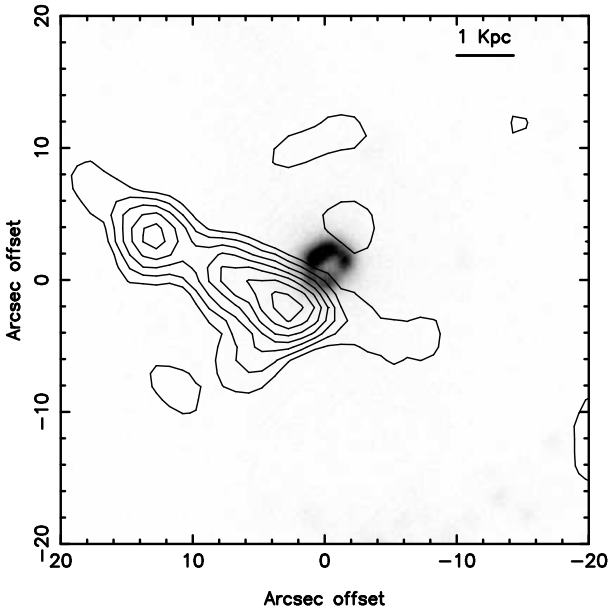

Figure 4. The Hα map taken from the AINUR atlas is plotted in gray scale. Overlaid on this map are the contours of the X-ray diffuse emission smoothed over 4 pixels. The contours are 5σ to 11σ times the noise level in steps of 1σ.

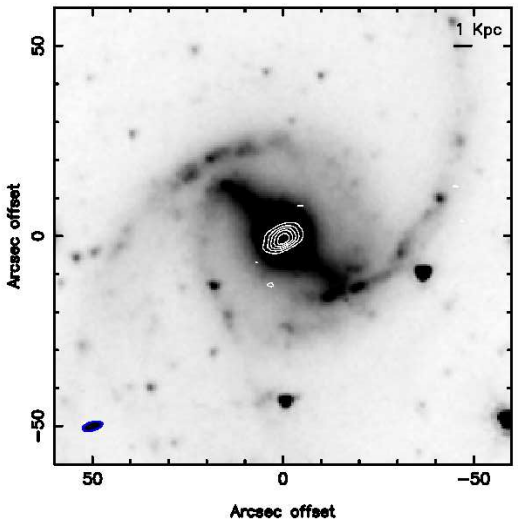

Figure 5. The figure shows the contours of radio continuum emission at 1280 Hz overlaid on the 3.6 micron IRAC near-infrared image of the galaxy. The contours are 5,10,15,20 and 25 times the noise level, which is 0.12 mJy/beam. The beam is elliptical and is 5.38″ × 2.21″; it is shown in the bottom left corner. The radio emission is concentrated about the nucleus within the small but bright bulge in the galaxy.

located near Pune, India (Ananthakrishnan & Pramesh Rao 2001). Nearby radio sources, 1438+621 and 3C 286, were used for phase and flux calibrations respectively. NGC 5905 was part of a larger survey of LSB galaxies and hence had a two hour scan. The data was obtained in the native ”lta” format, converted to FITS format and then analyzed using AIPS[2]. We obtained the 8 GHz radio data from the VLA archive. These observations were done during November, 1996. For this data, 1331+305 and 1510+570 were used as flux and phase calibrators respectively. The 1.4 GHz image that we have used was taken from VLA FIRST[3]; observations made during May, 1997. See Table 1 for more details.

We analyzed the radio continuum emission from NGC 5905 at the frequencies 8 GHz and 1280 Hz. For frequency 1435 Hz, we used the FIRST image. The 8 GHz VLA archival data was analyzed using AIPS but no source was detected and hence different resolution maps were not made. These observations were also analysed earlier (Komossa & Dahlem 2001) and a similar non-detection was obtained.

The GMRT 1280 GHz radio data was iteratively edited and calibrated until satisfactory gain solutions were obtained using standard tasks in AIPS. NGC 5905 was imaged used IMAGR; we made low resolution (robust 5) and high resolution (robust 0) maps. However, since our aim was to compare our GMRT flux density with the FIRST image (which has a beam of 5.4″ × 5.4″), we finally used the GMRT robust 0 map whose beam is similar and has a size of 5.38″ × 2.21″ (Figure 5). We convolved the GMRT map to the FIRST beam size i.e. 5.4″, using the AIPS task *CONVL*. The GMRT convolved flux density is 9.1 mJy. At all resolutions in the GMRT maps, the emission has a strong core but no extended structure; the source structure and flux density are similar to that of the FIRST image, whose compact source has a flux density of 8.95 mJy. The NVSS map has a flux density of 20.1 mJy which is significantly higher than both the FIRST and GMRT maps. But this may be due to its larger beam (45″) which picks up more of the extended diffuse emission.

2.3 Spitzer mid-infrared observation

The mid-infrared data were retrieved from the Spitzer archival spectroscopic observations (Program ID: ig-a02120140, PI: A. Zezas) obtained with the infrared spectrograph (IRS, Houck et al. 2004). The observations were taken with the short-high (SH) and long-high (LH) modules covering the spectral ranges 9.9 – 19.6 μm and 18.7 – 37.2 μm, respectively. The slit width was 4″.6 for SH and 9″.0 for LH. The observations were reduced as described in detail by Pereira-Santaella et al. (2010).

A high-resolution mid-infrared (mid-IR) spectrum of the nucleus of NGC 5905 was extracted using the IRS data. Figure 6 shows the plot of the IRS spectrum. There is no indication of any presence of the [NeV] lines at 14.3 and 24.3 μm in this spectrum. The 11.3micron PAH feature is detected and the measured value of the equivalent width (EW) of the feature is $\sim$ 0.8 μm. This value is typical of (high metallicity) star-forming galaxies (see Hernán-Caballero & Hatziminaoglou 2011).

3 RESULTS

3.1 Change in X-Ray Luminosity

The nuclear region of NGC 5905 is clearly detected in the X-ray and radio image of the source. The best fit model to the X-ray

[2] Astronomical Image Processing System (AIPS) is distributed by NRAO which is a facility of NSF and operated under cooperative agreement by Associated Universities, Inc.
[3] Faint Images of the Radio Sky at Twenty-Centimeters

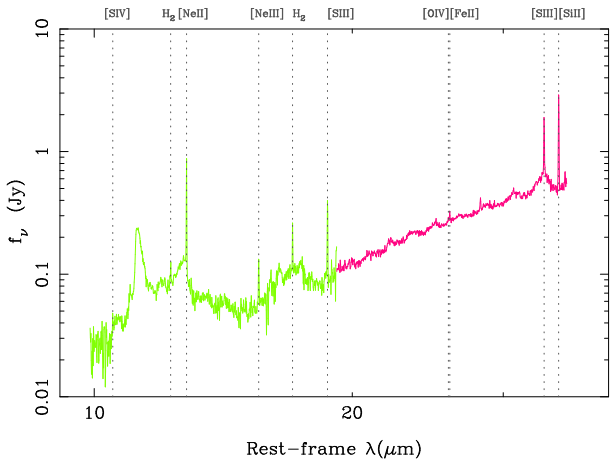

Figure 6. The figure shows the extracted high-resolution mid-infrared spectrum of NGC 5905. The position of prominent lines are marked on the top axis.

spectrum yields the X-ray flux of the source as $f_x = 1.5^{0.3}_{-0.2} \times 10^{-14}$erg s^{-1}cm^{-2} in the energy band of 0.3 – 8.0 keV (also see Table 2). We also tried other models, the details of which are presented in Table 2. The powerlaw model with variable N_H gives a very high value for the powerlaw index. A purely powerlaw model with absorption column density fixed to galactic value ($N_H = 1.5\times10^{20}$cm^{-2}) gives a very poor fit. We also try an absorbed blackbody model with variable and fixed N_H value but both the models give poor fit. Thus even though the soft X-ray part of spectrum (below 1 keV) is well described by a blackbody model the spectrum above 1 keV requires an additional powerlaw component. For comparison, the 0.5-2 keV X-ray luminosity of NGC 5905 during the 2007 Chandra observations is a factor of $\sim$ 200 less than the luminosity observed during the peak of the X-ray flare in 1990.

3.2 No type-I AGN signatures in X-Ray, IR or Radio emission

The X-ray image of NGC 5905 (Figure 2) does not show a centrally peaked source as is expected from an AGN. The nuclear X-ray emission is clearly visible in the 0.5-2.0 keV energy band and is very faint in the 2.0-7.0 keV energy band. The image does not show any bright central pixel about which the source counts decrease, rather the bright pixels are uniformly distributed within an almost circular region of radius about 0.05' (~700pc) (see Figure 2). If an AGN were present in the galaxy then a centrally bright source would be expected in the image at both the energy bands and the central source would be brighter in the 2.0-7.0 keV energy band image (Bauer et al. 2004).

The IR spectrum does not show any [NeV] lines at 14.3 or 24.3 μm which are expected if the galaxy hosts an AGN. The measured [OIV]25.89 μm/[NeII]12.81 μm ratio ($\simeq$ 0.025) indicates that the nuclear emission of this galaxy is probably powered by star formation (see Pereira-Santaella et al. 2010). On the other hand, the bright 11.3μm PAH feature and the [NeII] line at 12.81 μm line indicate that there is high star formation in the nuclear region of the galaxy. From the SFR calibration given in Diamond-Stanic & Rieke (2012) based on the [NeII] line we obtain a nuclear SFR (for a Salpeter IMF) of 2.3 $M_\odot$yr^{-1}, in good agreement with the estimate of Mazzuca et al. (2008) using Hα observations. Using the correlations between SFR and the soft X-ray luminosity of Pereira-Santaella et al. (2011) we get an expected 0.5-2.0 keV X-ray luminosity of $\sim 4 \times 10^{39}$erg s^{-1} consistent with the measured X-ray luminosity (see Table 2) leaving no excess X-ray emission which can be associated with a central Seyfert 2 type AGN.

The absence of radio emission in the 8 GHz VLA radio map also points to the absence of an AGN. The flux density of radio emission from AGNs does not fall as sharply with increasing frequency as star forming regions (Condon 1992). Hence if the compact radio core was due to an AGN, we would have observed some emission at 8 GHz as well.

Gezari et al. (2003) observed NGC 5905 in the optical using the HST/STIS which has a narrow slit size of 0''.1 and hence detected narrow emission lines from the nuclear region of the galaxy. But they did not detect any broad Balmer line emission. Furthermore, the spatial profile of the HST acqusition image obtained by them also does not indicate any AGN-like unresolved point source in the nucleus. Thus no evidence for a type-I AGN is found from X-ray, Optical, IR or radio data. We infer that any AGN present in NGC 5905 is very weak, as also indicated by a low total X-ray luminosity (see Table 2), and rule out the possibility that the RASS observed X-ray flare of 1990 in this galaxy was a result of large-amplitude variability in the Seyfert nucleus.

3.3 Change in radio flux density from 1996 to 2011 ?

To make an accurate comparison of the radio flux density in 1996 with that observed in 2011, we smoothed the GMRT map to the FIRST beam resolution and then used a typical spectral index value to normalize the flux densities to the same frequency. We smoothed the GMRT robust 0 map to the FIRST beam size (see Section 3.2) and then using a spectral index of $\alpha = -0.8$, which is typical of star forming regions and assuming that the intensity varies with frequency as $S_\nu \propto \nu^\alpha$, we determined the expected flux density at 1430 Hz. The GMRT flux density scaled to 1430 Hz is 8.31 mJy. The flux density in the FIRST 1997 image at 1430 Hz is 8.95 mJy, which is then only marginally higher (~7%) than that expected from the GMRT 2011 observations. The difference is within error limits on their flux densities. Thus the flux densities between 1997 and 2011 match fairly well and we conclude that there is no change in the nuclear radio emission from NGC 5905. Some models predict that radio jets may be triggered by the tidal disruption of a star and will give rise to a higher radio flux from the nucleus (Burrows et al. 2011). In NGC 5905 the tidally disrupted star that could have produced the X-ray flare is estimated to be relatively small in stellar mass (Li et al. 2002). Thus even if a radio jet had been launched, the emission due to such a jet may have been weak and would have decayed significantly by the time the FIRST observations in 1997 were made.

3.4 X-ray flare - signature of tidal disruption of a star

There has been a lot of analysis in the literature regarding the origin of X-ray flares from galaxies (Komossa 2005) and it is fairly clear now that either AGN activity or the tidal disruption of a star by a quiescent super massive black hole could cause a large X-ray flare like the one observed in NGC 5905. Since we find no clear signature of AGN activity in NGC 5905, either in optical, mid-infrared or radio emission, we conclude that the X-ray flare must be due to a tidal disruption event (Rees 1988). Thus the X-ray flare and the absence of AGN activity in this galaxy signifies the presence of a non-accreting BH in the galaxy nucleus.

3.5 Diffuse X-ray Emission - star formation or tidal debris ?

We have detected faint diffuse X-ray emission from within the bulge, about 2″ from the galaxy center. The AINUR Hα image of NGC 5905 shows the presence of a central ring of nuclear star formation (Comeron et al. 2010). Figure 4 is an overlay of the X-ray diffuse emission contours on this Hα map. Though there is no spatial correlation between the Hα and the diffuse X-ray emission, the X-ray emission seen may be due to star formation. Alternatively, it could be either the result of the interaction of a radio jet (launched due to the tidal disruption event) with the interstellar medium (Burrows et al. 2011) or the throw back tidal debris produced by a supernova like shell of shocked gas (Khokhlov & Melia 1996). It remains inconclusive that which of the above stated scenarios can result in the observed diffuse X-ray emission in NGC 5905 because of the lack of more photons in the available Chandra data. Deep X-ray observations and follow-up radio observations of such X-ray flares in galaxies can help us understand the post-tidal disruption evolution and confirm whether diffuse X-ray emission is indeed a by product of tidal disruption of stars by nuclear BHs.

4 CONCLUSION

1. No AGN in NGC 5905 : We have analysed Chandra X-ray, GMRT/VLA radio and the Spitzer mid-IR nuclear spectrum of NGC 5905. Our analysis suggests that there is no AGN in NGC 5905. Hence the X-ray flare observed by RASS in 1990-1991 is most likely due to the tidal disruption of a star by the nuclear black hole.

2. Change in X-ray Flux : The X-ray luminosity in the energy band 0.5 – 2.0 keV in 2007 Chandra data is $L_x = 3.2 \times 10^{39}$ ergs^{-1}. This is a factor of 200 less than the peak luminosity of the X-ray flare observed by RASS in 1990. But there seems to be no significant decrease in the X-ray flux from the 2002 Chandra observations (Halpern et al. 2004).

3. No Change in Radio Flux density : Comparing the FIRST VLA observations of 1997 with the GMRT radio observations in 2011, we find that there is no change in the radio flux density between 1997 and the 2011 epoch observations. The nucleus was not detected at 8 GHz in radio emission, which suggests that the spectral index is similar to that of star forming regions and not AGNs.

4. Diffuse X-ray Emission : We detected diffuse X-ray emission about 2″ away from the nucleus and just outside the circumnuclear ring of star formation. The emission could be associated with the star forming ring or alternatively it could arise from shocked gas which is formed by the interaction of a radio jet, triggered by the tidal disruption event, with the interstellar medium.

ACKNOWLEDGMENTS

We thank the GMRT staff for help in the observations. The GMRT is operated by the National Center for Radio Astrophysics of the Tata Institute of Fundamental Research. This research has made use of data obtained from the Chandra Data Archive and the Chandra Source Catalog, and software provided by the Chandra X-ray Center (CXC) in the application package CIAO. This work is based [in part] on observations made with the Spitzer Space Telescope, which is operated by the Jet Propulsion Laboratory, California Institute of Technology under a contract with NASA. This research has made use of the NASA/IPAC Extragalactic Database (NED) which is operated by the Jet Propulsion Laboratory, California Institute of Technology, under contract with the National Aeronautics and Space Administration. This work has also made use of the NRAO VLA FIRST image and the 8 GHz NRAO VLA Archival data of NGC 5905. M.D. would like to thank S. Komossa for very useful discussions regarding NGC 5905.

REFERENCES

Ananthakrishnan S., Pramesh Rao A., 2001, in 2001 Asia-Pacific Radio Science Conference AP-RASC '01 The Indian Giant Metrewave Radio Telescope (invited). p. 237
Bade N., Komossa S., Dahlem M., 1996, A&A, 309, L35
Bauer F. E., Alexander D. M., Brandt W. N., Schneider D. P., Treister E., Hornschemeier A. E., Garmire G. P., 2004, AJ, 128, 2048
Bower G. C., Metzger B. D., Cenko S. B., Silverman J. M., Bloom J. S., 2013, ApJ, 763, 84
Burrows D. N., Kennea J. A., Ghisellini G., Mangano V., Zhang B., Page K. L., Eracleous M. e. a., 2011, Nature, 476, 421
Cappelluti N., Ajello M., Rebusco P., Komossa S., Bongiorno A., Clemens C., Salvato M., Esquej P., Aldcroft T., Greiner J., Quintana H., 2009, A&A, 495, L9
Comeron S., Knapen J. H., Beckman J. E., Laurikainen E., Salo H., Martínez-Valpuesta I., Buta R. J., 2010, MNRAS, 402, 2462
Condon J. J., 1992, ARA&A, 30, 575
Das M., Reynolds C. S., Vogel S. N., McGaugh S. S., Kantharia N. G., 2009, ApJ, 693, 1300
Diamond-Stanic A. M., Rieke G. H., 2012, ApJ, 746, 168
Donley J. L., Brandt W. N., Eracleous M., Boller T., 2002, AJ, 124, 1308
Esquej P., Saxton R. D., Freyberg M. J., Read A. M., Altieri B., Sanchez-Portal M., Hasinger G., 2007, A&A, 462, L49
Esquej P., Saxton R. D., Komossa S., Read A. M., 2012, in European Physical Journal Web of Conferences Vol. 39 of European Physical Journal Web of Conferences, Tidal disruption events from the first XMM-Newton slew survey. p. 2004
Gezari S., Basa S., Martin D. C., Bazin G., Forster K., Milliard B., Halpern J. P., Friedman P. G., Morrissey P., Neff S. G., Schiminovich D., Seibert M., Small T., Wyder T. K., 2008, ApJ, 676, 944
Gezari S., Halpern J. P., Komossa S., Grupe D., Leighly K. M., 2003, ApJ, 592, 42
Gezari S., Heckman T., Cenko S. B., Eracleous M., Forster K., Gonçalves T. S., Martin D. C., Morrissey P., Neff S. G., Seibert M., Schiminovich D., Wyder T. K., 2009, ApJ, 698, 1367
Giuricin G., Bertotti G., Mardirossian F., Mezzetti M., 1990, MNRAS, 247, 444
Gültekin K., Richstone D. O., Gebhardt K., Lauer T. R., Tremaine S., Aller M. C., Bender R., Dressler A., Faber S. M., Filippenko A. V., Green R., Ho L. C., Kormendy J., Magorrian J., Pinkney J., Siopis C., 2009, ApJ, 698, 198
Halpern J. P., Gezari S., Komossa S., 2004, ApJ, 604, 572
Hernán-Caballero A., Hatziminaoglou E., 2011, MNRAS, 414, 500
Ho L. C., 2008, ARA&A, 46, 475
Ho L. C., Filippenko A. V., Sargent W. L., 1995, ApJS, 98, 477
Ho L. C., Greene J. E., Filippenko A. V., Sargent W. L. W., 2009, ApJS, 183, 1
Houck et al. J. R., 2004, ApJS, 154, 18
Kent S. M., 1985, ApJS, 59, 115

Khokhlov A., Melia F., 1996, ApJ, 457, L61
Komossa S., 2005, in Merloni A., Nayakshin S., Sunyaev R. A., eds, Growing Black Holes: Accretion in a Cosmological Context Growing Black Holes: Observational Evidence for Stellar Tidal Disruption Events. pp 159–163
Komossa S., Bade N., 1999, A&A, 343, 775
Komossa S., Dahlem M., 2001, ArXiv Astrophysics e-prints
Kuzio de Naray R., McGaugh S. S., de Blok W. J. G., 2008, ApJ, 676, 920
Li L.-X., Narayan R., Menou K., 2002, ApJ, 576, 753
Maksym W. P., Ulmer M. P., Eracleous M., 2010, ApJ, 722, 1035
Mayer L., Wadsley J., 2004, MNRAS, 347, 277
Mazzuca L. M., Knapen J. H., Veilleux S., Regan M. W., 2008, ApJS, 174, 337
Naik S., Das M., Jain C., Paul B., 2010, MNRAS, 404, 2056
Norman C., Silk J., 1983, ApJ, 266, 502
Pereira-Santaella M., Alonso-Herrero A., Santos-Lleo M., Colina L., Jiménez-Bailón E., Longinotti A. L., Rieke G. H., Ward M., Esquej P., 2011, A&A, 535, A93
Pereira-Santaella M., Diamond-Stanic A. M., Alonso-Herrero A., Rieke G. H., 2010, ApJ, 725, 2270
Pizzella A., Corsini E. M., Dalla Bontà E., Sarzi M., Coccato L., Bertola F., 2005, ApJ, 631, 785
Ramya S., Prabhu T. P., Das M., 2011, MNRAS, 418, 789
Rees M. J., 1988, Nature, 333, 523
Saxton R. D., Read A. M., Esquej P., Komossa S., Dougherty S., Rodriguez-Pascual P., Barrado D., 2012a, A&A, 541, A106
Saxton R. D., Read A. M., Esquej P., Komossa S., Dougherty S., Rodriguez-Pascual P., Barrado D., 2012b, A&A, 541, A106
Sprayberry D., Impey C. D., Bothun G. D., Irwin M. J., 1995, AJ, 109, 558
van Moorsel G. A., 1982, A&A, 107, 66
Walker M. G., McGaugh S. S., Mateo M., Olszewski E. W., Kuzio de Naray R., 2010, ApJ, 717, L87